https://doi.org/10.3311/PPch.42739

Periodica Polytechnica Chemical Engineering, 70(1), pp. 113–123, 2026

Application of Design Experiments in Optimizing Silica Extraction from Coal Fly Ash and the Product Characterization

Devy Cendekia[1], Widi Astuti[2], Eko Sri Kunarti[1], Nuryono Nuryono[1*]

[1] Department of Chemistry, Faculty of Mathematics and Natural Sciences, Universitas Gadjah Mada, Sekip Utara 55281, Indonesia
[2] Research Center for Mineral Technology, Ir. Sutami street Km. 15, Tanjung Bintang, South Lampung, Lampung 35361, Indonesia
* Corresponding author, e-mail: nuryono_mipa@ugm.ac.id

Received: 10 November 2025, Accepted: 16 February 2026, Published online: 17 March 2026

Abstract

Mesoporous silica was successfully extracted from coal fly ash using the sol-gel method at optimum temperature and stirring speed. To optimize conditions for silica extraction the temperature response and stirring speed were analyzed using Design-Expert software with a central composite design under response surface methodology. The study yielded optimal conditions at 80 °C and 260 rpm. The ideal response under these circumstances yielded 7.8% coal fly ash silica (SCFA). Fourier transform infrared spectroscopy analysis results showed that the SCFA had a wavelength of specific silica compounds at 1013 cm^{-1}, which is the result of intermittent strain vibrations caused by Si–O–Si. Surface analysis by scanning electron microscope - energy dispersive X-ray spectroscopy reveals that the SCFA material has a relatively rough, porous surface, dominated by silicon and aluminum. The SCFA is a mesoporous material with a large surface area of 223 m^2/g , a total pore volume of 0.45 cm^3/g and an average pore diameter of 7.8–8.1 nm. Overall, the characterization results indicate that SCFA has a large surface area, a stable mesoporous structure and a chemical composition dominated by SiO_2 (93.35%). These characteristics make the material a promising candidate for use as a metal adsorbent, catalyst media and functional material in field environments and industries.

Keywords

silica, coal fly ash, RSM, mesopores

1 Introduction

Coal fly ash (CFA) is a byproduct of the pulverized coal combustion process in thermoelectric power plants. Only about 5% of CFA is recycled in the cement and construction industries. Due to its high silicon and aluminum content, CFA represents a valuable secondary resource of pure silica and alumina. Silica has high economic value due to its widespread use in various industrial applications, including as catalysts and catalyst supports, pigments, electronic substrates, thin-film substrates, electrical and thermal insulators, exhaust gas filters and adsorbents [1, 2].

Pollution from CFA has a negative impact; however, fly ash derived from coal contains high levels of silica, alumina and iron, which are also commonly present in fly ash after combustion. Over the last decade, technological advancements in nanotechnology and the development of nanoparticles have enabled the creation of applications in various fields, including catalysis, drug delivery, medicine and other chemical industries. However, nanoparticle synthesis requires expensive precursor materials and sophisticated instruments, making the final nanoparticles very expensive. Therefore, nanotechnology utilizes waste materials, including agricultural waste (such as bagasse and rice husk ash) and industrial waste (such as geothermal waste, red mud and fly ash), as inexpensive precursors.

The synthesis of nanoparticles from agricultural waste or industrial waste can help minimize solid waste as a source of pollution. One precursor for synthesizing silica, alumina, and iron nanoparticles is fly ash. Fly ash is a rich source of silica (40–60%), alumina (20–40%), iron (5–15%) and calcium (0.5–15%), depending on the type of coal used, its geographic origin and the operating conditions for coal combustion in thermal power plants [3]. One source of silica that can be utilized is CFA waste. The silica derived from CFA has potential as a hydrogen storage material because its pore diameter exceeds 0.7 nm. It can reach a purity of up to 87%, and it demonstrates excellent thermal

Cite this article as: Cendekia, D., Astuti, W., Sri Kunarti, E., Nuryono, N. "Application of Design Experiments in Optimizing Silica Extraction from Coal Fly Ash and the Product Characterization", Periodica Polytechnica Chemical Engineering, 70(1), pp. 113–123, 2026. https://doi.org/10.3311/PPch.42739

stability, especially between 120–300 °C; therefore, it could serve as a catalyst in the hydrogen adsorption-desorption process with magnesium [4].

Generally, SiO_2 can be obtained from both inorganic and organic materials. SiO_2 is chemically stable, insoluble in water, and resistant to high temperatures. Mesoporous silica nanoparticles can be produced from sodium silicate precursors extracted from coal fly ash through a direct alkaline leaching (DAL) process consisting of a one-step element extraction from fly ash using NaOH. Silica is a mineral compound composed primarily of silicon oxide. Silica is widely used in various industrial applications, including catalysts, pigments, pharmaceuticals, electronics, thin films, heat insulators and humidity sensors. Natural silica from biomass can be used to catalyze MgH_2. The characteristics of hydrogen storage, such as temperature and desorption time, have been enhanced by simultaneously employing nickel and silica as dual catalysts. Nickel and silicon oxide catalysts were used to reduce the operating temperature of MgH_2 [5, 6].

Some typical silica syntheses employ chemical methods, including sol-gel, microemulsion and hydrothermal/solvothermal routes. However, the most commonly used method is the sol-gel process. This method is considered more effective for producing silica products with high purity and homogeneity, and it allows control over pore size and distribution [7]. The sol-gel technique is relatively low-cost, operates mild reaction conditions, and offers flexibility in tailoring the composition and structure of silica-based materials [8].

Pure silica (≈90% purity) is produced through solid-liquid extraction followed by leaching, a diffusion-based purification process influenced by factors such as particle size, solvent type, temperature, and stirring speed [9]. In this study, the optimization of operating temperature and stirring speed will be conducted to achieve silica purity.

The silica production process typically involves treating the ash with NaOH under reflux conditions, then centrifuging and precipitating with HCl. The pH of the solution significantly affects the SiO_2 content obtained, with the highest results observed at pH 10 [10]. Pretreatment with acid solutions is also widely applied to remove impurities before mixing with NaOH and heating, producing sodium silicate with the main chemical composition of SiO_2, Al_2O_3, CaO, and Fe_2O_3 [11]. Another method involves treating a mixture of CFA and $CaCO_3$ at high temperature (1200 °C) before acid treatment with HCl, which shows that acid concentration, temperature and time influence Si recovery [12].

Spectroscopic analysis, various hydrothermal, alkaline digestion strategies and response surface methodology (RSM) have been applied in previous studies to extract Si and Al from coal fly ash and agricultural wastes, revealing the strong influence of parameters such as temperature, NaOH concentration and reaction time on silica recovery and subsequent material synthesis [13]. These works consistently demonstrate that temperature is the most dominant factor governing silica extraction efficiency, followed by alkaline concentration and processing duration, with optimized conditions enabling successful conversion of extracted species into high-value products such as zeolites [14].

RSM is an essential tool for process optimization because it provides insights into how factors like temperature and solvent-to-solid ratio influence extraction yield [11]. RSM was used in this study to build a prediction model that would maximize the extraction procedure. To model and optimize silica extraction from CFA, this study combines a hydrodynamic parameter (stirring speed) with citric acid as a green pretreatment agent. Therefore, this work aims to model and optimize the silica extraction process using temperature and stirring speed as key variables, and characterize the purified silica obtained under the optimized conditions.

2 Materials and methods

2.1 Material

The CFA sample was obtained from the Tarahan Steam Power Plant, Lampung, Indonesia. Sodium hydroxide (analysis-grade pellets) was obtained from Merck (Darmstadt, Germany). Hydrochloric acid (37% purity, analytical reagent grade) was supplied by Smart-Lab, Tangerang, Indonesia. Citric acid (Wako Pure Chemicals Industries, Ltd., Tokyo, Japan) and distilled water were used.

2.2 Sample preparation

The sample used in this study was CFA waste with a particle size of 0.15 mm. The sieved particles were dried at 100 °C for 105 min. The pretreatment process was initiated by mixing 20 g of sieved CFA with 80 mL of 20% citric acid solution, corresponding to a solid-to-acid volume ratio 1:4. The mixture was stirred until a homogeneous slurry was formed, after which it was filtered and thoroughly washed with distilled water until the filtrate reached a pH comparable to that of the initial distilled water, indicating the removal of residual acid. The washed solids were then dried in an oven at 60 °C until a constant mass was achieved, confirming the completion of moisture removal [9]. The acid-treated

CFA was subsequently subjected to silica extraction using the sol-gel method to isolate the silica fraction. In the sol-gel process, the sample (20 g) was reacted with 2 M NaOH (80 mL) (mass to volume ratio 1:4) and stirred with a magnetic stirrer at a specified temperature and stirring speed. The filtrate obtained was dripped with 1 M HCl until a gel was formed, and the resulting colloidal gel was left for 18 h. The next step was washing with demineralized water and drying at 60 °C for 18 h. The yield of the product relative to the silica leached from the leaching process was then determined using Eq. (1). In this study, the silica yield was defined as the mass of extracted silica relative to the mass of the acid-treated CFA.

$$\text{yield} = \frac{\text{mass of silica}(\text{g})}{\text{mass of sample}(\text{g})} \times 100\% \quad (1)$$

2.3 Experimental setup for optimizing the extraction

The silica yield in the sol-gel extraction process can be increased by controlling the stirring speed and the operating temperature. This study employed two factors: stirring speed (200–400 rpm) and operating temperature (60–80 °C), to optimize silica extraction. The experiment was conducted according to the settings outlined in Table 1, utilizing Design-Expert 13.0.5.0 software (Stat-Ease, Inc.). The results of the software analysis were used to determine the optimal response for producing silica from coal fly ash.

Silica was extracted from CFA using the sol-gel method. The CFA samples after the pretreatment stage were extracted with 2 M NaOH at a feed-to-solvent ratio 1:4, with stirring speed and operating temperature determined using a central composite design (CCD) with RSM. Table 2 presents the CCD experimental setup designed using Design-Expert software. The experiment was conducted in 12 runs, and the software was used to analyze the experimental response using ANOVA based on p-values at a 95% confidence level.

2.4 Validation experiment

Validation experiments were conducted to validate the optimal conditions suggested by the Design-Expert software.

Table 1 Ranges for factorial analysis

Factor	Range	
	Low level	High level
Mixing speed (rpm)	200	400
Temperature (°C)	60	80

Table 2 Experimental design settings with Design-Expert software

Run	Factor 1 A: stirring speed (rpm)	Factor 2 B: temperature (°C)
1	400	80
2	300	70
3	300	84
4	300	70
5	200	80
6	300	55
7	441	70
8	200	60
9	400	60
10	158	70
11	300	70
12	300	70

The criteria for selecting optimal conditions included stirring speed and operating temperature to maximize silica extract yield. Optimal experimental conditions are those that produce the maximum yield and the highest

2.5 Characterization methods

Products are characterized using the following methods: Fourier transform infrared spectroscopy (FTIR; 670 Plus spectrophotometer, JASCO, Tokyo, Japan); scanning electron microscope - energy dispersive X-ray spectroscopy (SEM-EDS; VE-9800 SEM, Keyence, Osaka, Japan, and EDAX Genesis, Ametek, NJ, USA); X-ray diffractometry (XRD; Ultima IV, Rigaku, Tokyo, Japan; X-Ray fluorescence (XRF; ZSX Primus II, Rigaku, Tokyo, Japan) and low temperature nitrogen adsorption adsorption (Micromeritics Tristar II Plus; Micromeritics Instrument Corp; Norcross; USA) analysis.

3 Results and discussion

In this study, 12 experiments were conducted to investigate silica extraction from coal fly ash, and the producing of silica from coal fly ash (SCFA) using different factor combinations. The silica extraction process uses the sol-gel method using an alkaline solution. Silica is highly soluble in solutions with a pH greater than 10. Acidification is also required in the production of silica gel. This method has several advantages, including being cheaper and less environmentally harmful than quartz melting techniques [15]. At the beginning of the experiment, the CFA sample underwent a leaching stage with citric acid to dissolve metal oxides and organic impurities, producing high-purity silica. The H^+ ions from the acid bind with oxygen

from the metal oxide that has previously been separated. The reaction mechanism during the leaching stage involving the oxide compound is shown in Eq. (2). The letter X in the reaction equation indicates the metal element present in the sample, for example, iron.

$$C_6H_8O_7(aq) + X_2O_3 \rightarrow X_2(C_6H_2O_7) + 3H_2O \quad (2)$$

The acid-leached sample appears lighter in color than the initial sample (Fig. 1(a)). This may be due to the release of impurities, such as metal oxides, from the sample during the leaching process [16].

In the next stage of silica recovery, two steps are employed: the formation of a sodium silicate sol using NaOH in the first stage, followed by gelation with HCl. In the first stage, NaOH is used to dissolve the silica compound by stirring it into a sodium silicate compound, as shown in Eq. (3). In this study variations in stirring speed and temperature were conducted to determine the effects on the characteristics of the results obtained during the characterization stage, specifically the chemical bonds that form.

$$SiO_2 + 2NaOH \rightarrow Na_2SiO_3 + H_2O \quad (3)$$

The sodium silicate precursor formed is then used in the second stage, namely in the gelation process, to reform the SiO_2 compound. The stages in this process are condensation to form silicic acid, $Si(OH)_4$, into cyclic oligomers, which then polymerize into a three-dimensional structure. The sodium silicate precursor was aged for 24 h, and a silica precipitate formed. This precipitation process is a condensation event, and the formation of silica gel particles [17]. During aging, the colloidal particles will form a transparent precipitate. The reactions that occur in the second process are shown in Eq. (4)-(5) [18].

$$Na_2SiO_3 + 2HCl + H_2O \rightarrow Si(OH)_4 + 2NaCl \quad (4)$$

$$n\left[Si(OH)_4 + (OH)_4Si\right] \rightarrow n[\equiv O - Si - O \equiv] + 2nH_2O \quad (5)$$

Experiments were conducted to determine the optimal point by varying the stirring speed and operating temperature factors. The response of silica yield values to the given factors are shown in Table 3.

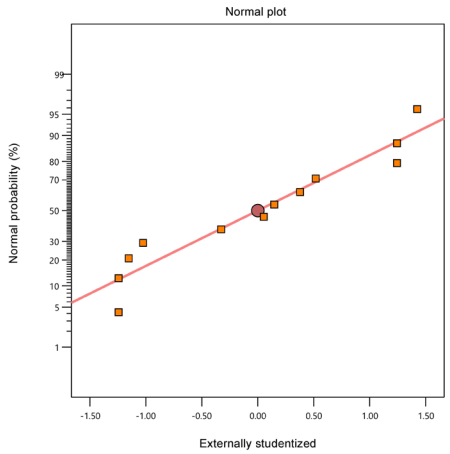

(a)

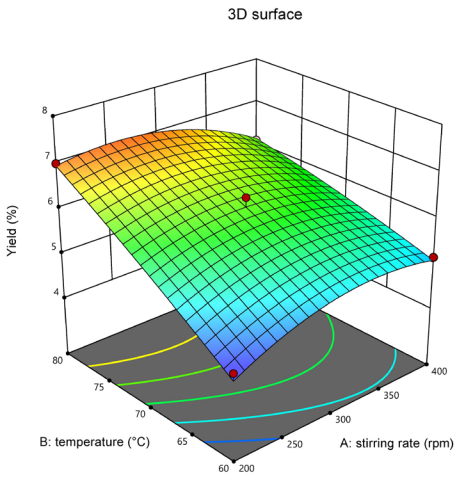

(b)

Fig. 1 (a) Comparison of predicted data distribution versus actual silica yield response data; (b) 3D diagram of the surface response showing the interaction between factors (stirring rate and temperature) and the response (silica yield)

3.1 Analysis of variance

3.1.1 Response surface methodology model development and analysis of variance

The analysis of variance (ANOVA) summary for the silica yield is presented in Table 4. In the ANOVA table, the degree of freedom (df) indicates the number of independent contributions of each factor to the variation in silica yield. The model df reflects the inclusion of temperature,

Table 3 Analysis results of silica extraction using the sol-gel method

No	Factor 1 A: stirring speed (rpm)	Factor 2 B: temperature (°C)	Response yield (%)
1	400	80	6.10
2	300	70	6.36
3	300	84	7.32
4	300	70	5.95
5	200	80	6.99
6	300	55	4.61
7	441	70	5.23
8	200	60	4.57
9	400	60	5.15
10	158	70	5.19
11	300	70	5.95
12	300	70	6.36

Table 4 ANOVA analysis for silica yield

Source	Sum of squares	df	Mean square	*F*-value	*p*-value	Annotation
Model	8.32	5	1.66	41.44	0.0001	Significant
A-stirring speed	0.01	1	0.01	0.18	0.6844	
B-temperature	6.50	1	6.50	162.03	< 0.0001	
AB	0.55	1	0.55	13.60	0.0102	
A^2	1.26	1	1.26	31.29	0.0014	
B^2	0.03	1	0.03	0.70	0.4343	
Residual	0.24	6	0.04			
Lack of Fit	0.07	3	0.02	0.4110	0.7578	Not significant
Pure Error	0.17	3	0.06			
total corrected sum of squares	8.56	11				

stirring speed, their interaction and quadratic terms, while the residual df represents the experimental error obtained from replicated runs. The *p*-value for the resulting model is 0.0001; a *p*-value less than 0.05 indicates that the model is significant. The correlation coefficient (R^2) value for the silica yield response is 0.9719, indicating that the model is acceptable and can represent the existing process [19]. The R^2 is a measure of the strength of the linear relationship between two variables. An R^2 value approaching −1 or +1 indicates a strong relationship between the two variables, and an R^2 value approaching 0 indicates a weak relationship between the two variables [20].

The ANOVA results for silica yield (Table 4) indicate that the quadratic model is statistically significant ($p < 0.0001$) and that the lack-of-fit is non-significant ($p = 0.4110$), confirming the adequacy of the model for process optimization. Temperature (A), the interaction between temperature and stirring speed (AB), and the quadratic term of temperature (A^2) were identified as significant factors ($p < 0.05$), highlighting the dominant role of thermal effects and hydrodynamic interactions in controlling silica leaching.

Temperature had a significantly higher *F*-value than stirring speed in the ANOVA data, suggesting that it is the primary factor affecting silica yield during extraction. Although the stirring speed's low *F*-value indicates a small direct effect, its strong interaction with temperature shows that hydrodynamic conditions still affect process efficiency. These findings show that stirring speed has a secondary but complementary function in silica extraction, which is largely controlled by heat factors. The strong influence of temperature is attributed to enhanced dissolution kinetics; at the same time, increased stirring speed improves mass transfer between the solid and liquid phases, thereby increasing silica extraction efficiency.

3.1.2 Interaction plots and response surface analysis

Fig. 1(a) illustrates that the actual data align with the predicted data, enabling analysis of the two-factor test results. The *x*-axis in Fig. 1(a) shows the actual data in the study, and the *y*-axis represents the predicted data in the application. In the distribution of silica yield response data, the points approach a linear line, indicating that the actual and predicted data do not differ significantly.

Fig. 1(b) illustrates the combined effect of temperature and stirring speed on silica yield, where ANOVA results identify temperature as the most influential parameter. At a constant stirring speed of 200 rpm, increasing the temperature leads to a higher silica yield. Higher temperatures enhance solubility and molecular mobility, allowing solvent molecules to penetrate the material matrix more effectively and promote target compound dissolution. Consequently, accelerated diffusion from the solid phase to the solvent increases the overall extraction rate [20]. Excessively low temperatures limit ion mobility and solvent penetration, whereas higher temperatures promote more effective disruption of the aluminosilicate matrix, thereby facilitating silica [22].

Numerical optimization using a CCD-based RSM model identified optimal conditions of 80 °C and 260 rpm, yielding a silica yield of 7.3%. This result is comparable to the approximately 7% yield reported in previous studies using alkaline extraction with 4 M NaOH under microwave irradiation at 10% power for 6 min [14]. Model validation confirmed good agreement between predicted and experimental values, with an accuracy exceeding 98%, demonstrating the reliability of the proposed RSM model (Table 5). Model validity was evaluated by comparing the predicted value with the average of three replicate experimental results obtained under optimal conditions [23].

Table 5 Results of validation experiment accuracy on silica yield values

Parameter	Lowest prediction	Prediction	Highest prediction	Verification results	Difference	Accuracy
Yield (%)	6.6389	7.0800	7.52095	7.37254	0.29254	96.03%

3.2 Characterization of silica coal fly ash

3.2.1 Fourier transform infrared analysis for functional group identification

The silica coal fly ash (SCFA) solid material obtained from the CFA extraction was characterized to identify the compounds successfully extracted. Fig. 2 shows the FTIR spectra of CFA and SCFA. The less clear CFA spectrum indicates that the silica structure is not yet dominant or is mixed with crystalline phases. The FTIR spectra of SCFA measurements were performed over the range of 4000–300 cm^{-1} to identify specific silica compounds. The band at 432.03 cm^{-1} is the vibration network of O−Si−O, while the band at 783 cm^{-1} is the symmetric stretching vibration of Si−O−Si [24]. The bands at 541 cm^{-1} and 675 cm^{-1} represent the bending vibration of Si−O [25].

The specific FTIR signal of silica particles was found at 1012 cm^{-1}, which is the result of intermittent stretching vibrations caused by Si−O−Si. The stretching vibration of the O−H bond of the silanol Si−OH group, caused by H_2O molecules adsorbed on the silica surface, gives rise to the band observed at 3376 cm^{-1}. The SCFA spectra produce stronger peaks than the CFA spectra, indicating a greater presence of surface −OH groups. This shows that the silica surface (Si−OH, silanol) is formed after leaching and extraction. Bending vibration of the O−H bond of the Si−OH silanol group gives rise to a vibration band at 1632 cm^{-1}; this is not clearly visible in CFA [26].

3.2.2 Crystallinity of silica coal fly ash

The XRD patterns were collected using Cu Kα radiation (λ = 1.540 Å), at 40 kV and 20 mA, over a 2θ range of 10° to 90°, to determine the crystal structure of the CFA material. Fig. 3 shows the difference in crystal phase of CFA and SCFA samples. Analysis of CFA samples reveals the

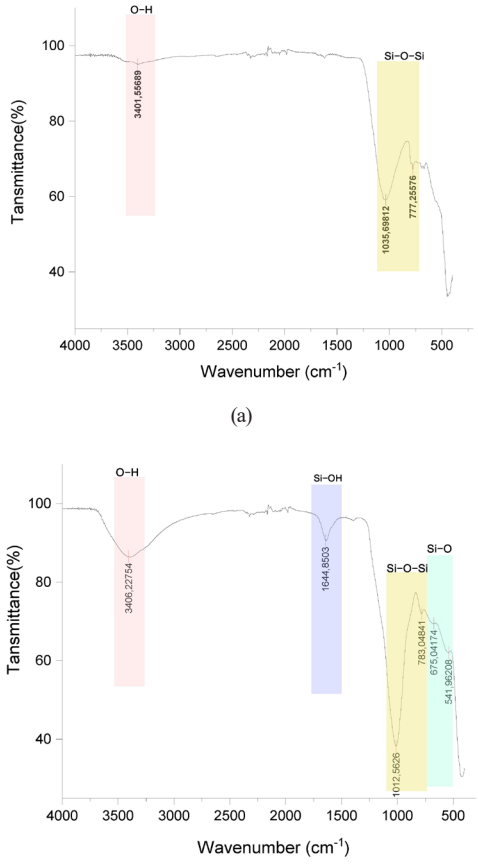

Fig. 2 FTIR spectra of (a) coal fly ash (CFA) and (b) silica coal fly ash (SCFA)

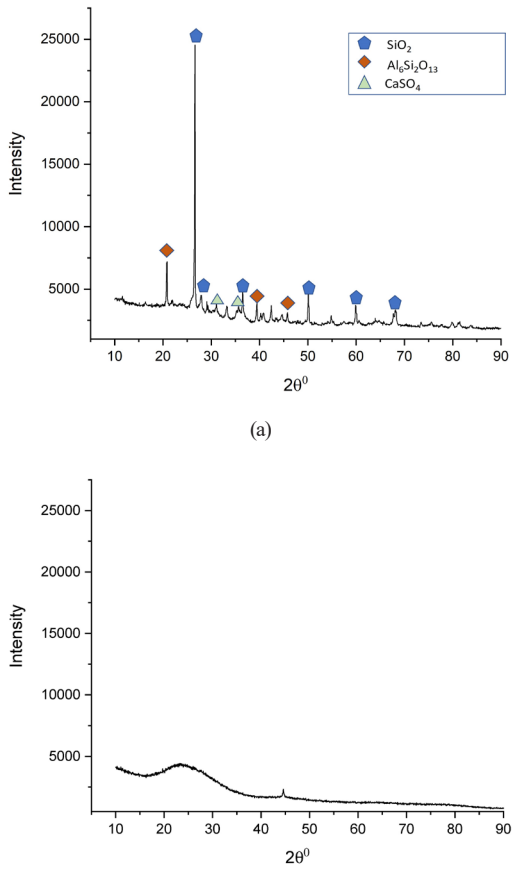

Fig. 3 XRD patterns of (a) coal fly ash (CFA) and (b) silica coal fly ash (SCFA)

presence of anhydrite ($CaSO_4$), mullite ($Al_6Si_2O_{13}$) and quartz (SiO_2), which are the crystal phases that make up the CFA sample. The diffraction pattern of the SCFA sample shows a broad diffraction peak centered at diffraction angle 2θ approximately 22°, which is characteristic of an amorphous structure [27]. The figure shows a broad peak at approximately 22°, indicating the abundance of amorphous silica in the matrix. The obtained SCFA particles were confirmed to be amorphous silica, as evidenced by their broad diffraction peaks [28].

The presence of a broad, diffuse peak centered at 20°–30°, with a maximum at $2\theta \approx 22°$, indicates the characteristic amorphous nature of silica. Similar XRD patterns have been reported in previous studies employing acid reflux processes, in which the complete removal of crystalline phases originating from active coal fly ash led to the appearance of a broad amorphous phase [29]. The present results still show minor aluminosilicate peaks (sodium aluminum silicate and sodalite), indicating their partial susceptibility to acid leaching.

3.2.3 Scanning electron microscopic analysis

SEM analysis was conducted to assess the success of the extraction process by examining surface differences between CFA and SCFA. The images were acquired at an accelerating voltage of 10 kV in secondary electron mode, with a magnificationof 5,000×. Fig. 4(a) shows the SEM image of CFA in the form of small and aggregated, with no regular shape, and with parts shaped almost round. The surface particles appear rough and porous,

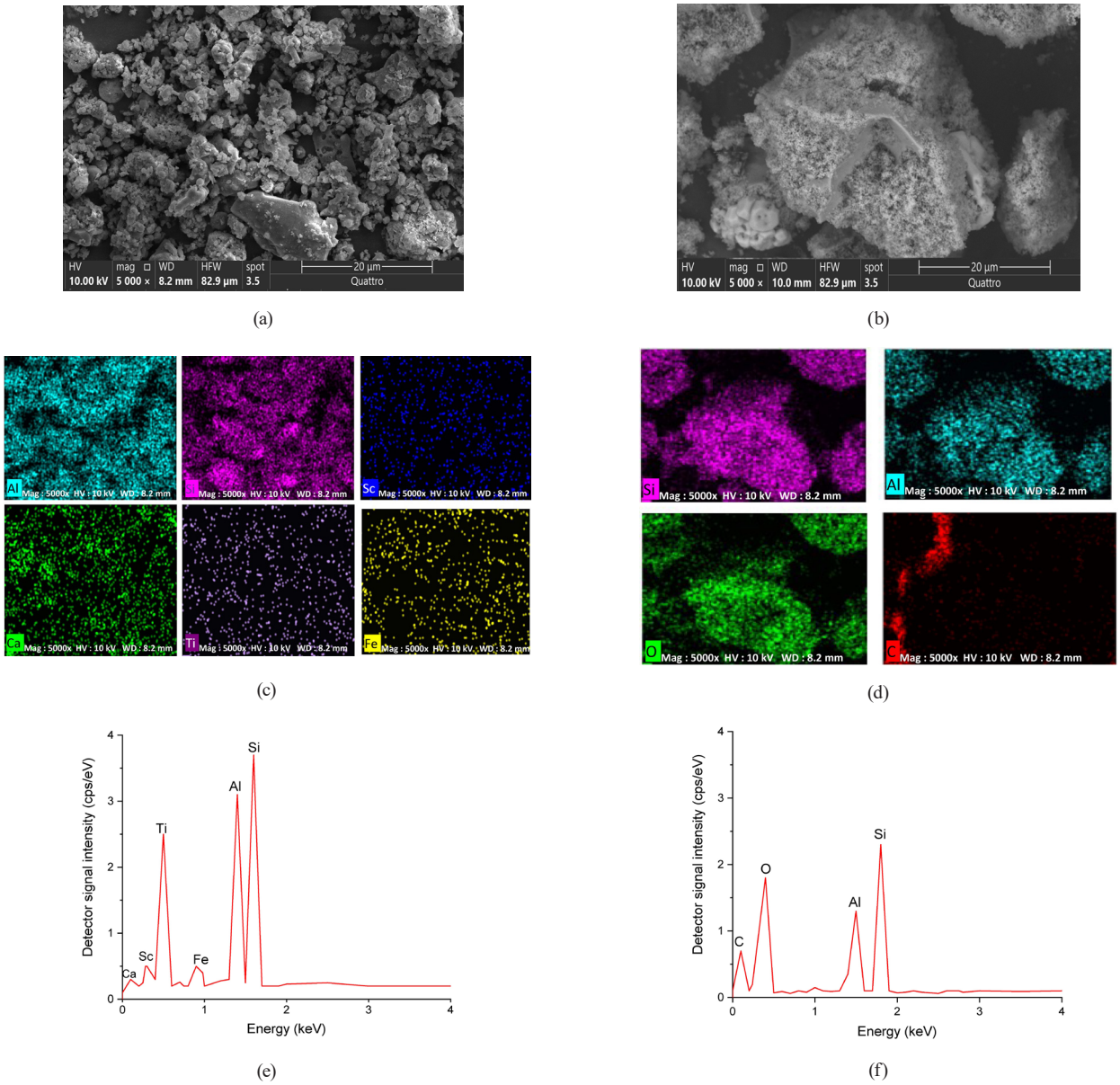

Fig. 4 SEM images of (a) CFA and (b) SCFA particles. Element mapping of (c) CFA and (d) SCFA particles. EDS graph of (e) CFA and (f) SCFA particles

suggesting a potentially large surface area (suitable for adsorbents/catalysts). In contrast, the SCFA particles (Fig. 4(b)) exhibit larger, angular morphologies with a more compact and granular surface texture. The appearance of surface hollows and fractures indicates significant structural modification induced by the extraction process, reflecting the removal of loosely bound phases and changes in particle integrity.

The elemental composition of CFA and SCFA samples was further examined using elemental mapping images (Figs. 4(c) and 4(d)), which confirm the dominance of O, Si, and Al, consistent with an aluminosilicate-based material. The corresponding elemental mapping images reveal that Si and O are broadly distributed across the observed areas, supporting the formation of a silica-rich matrix after extraction. Minor elements such as Al, Ti and Fe are detected with localized distributions, indicating their presence as residual phases rather than major constituents of the SCFA tructure. Based on FTIR, XRD and SEM-EDS-mapping analyses the SCFA material is amorphous silica, making it suitable for use as an adsorbent.

3.2.4 Composition of coal fly ash and silica coal fly ash

The results of the comparative EDS analysis for CFA and SCFA, as shown in Figs. 4(e) and 4(f), indicate that the CFA sample contains the dominant elements Si and Al, as well as minor elements Fe, Ca, Ti and Sc. The composition is complex, with an oxide mixture of SiO_2 and Al_2O_3, indicating its characteristic nature. Typically fly ash is rich in silica and alumina with metallic impurities (Fe, Ti). The SCFA sample shows that the dominant elements are Si (29.65%) and O (28.63%). The presence of Si and O components reaches almost 60%, indicating the existence of dominant SiO_2. The Al content declines from 16% to 6%, and minor elements (Fe, Ca, Ti and Sc) are almost depleted, indicating successful purification of silica (Table 6). The oxide composition was determined by XRF and reported as oxide weight percentages (wt.%).

Table 6 XRF analysis of oxide composition (wt.%) in CFA and SCFA materials

Oxide	Quantity (%)	
	CFA	SCFA
Al_2O_3	19.03	4.67
SiO_2	53.14	93.35
K_2O	1.11	0.36
CaO	8.93	0.34
Fe_2O_3	11.56	0.13

XRF analyzed the purity of the silica in the SCFA material. It reveals that SiO_2 is the primary component of SCFA, with other components serving as impurities. This indicates that the optimal conditions of the RSM analysis, as determined in the silica extraction process from CFA, yield silica purity above 90%.

In this study, process optimization using a 30-min extraction at 80 °C and a stirring speed of 260 rpm yielded silica with a purity of 93.35%. This performance surpasses that reported in prior work, where a 4 h contact time produced silica with a purity of only 87%, and another study in which a 2 h extraction resulted in 72% purity [4]. These findings highlight the effectiveness of employing citric acid during the pretreatment stage and demonstrate the significant enhancement in silica extraction efficiency achieved through process optimization using RSM.

3.2.5 Low temperature nitrogen adsorption analysis

The surface area analysis of SCFA was conducted to evaluate the solid surface capacity to adsorb gas molecules. According to the Brunauer–Emmett–Teller (BET) theory, N_2 molecules can be adsorbed in multiple layers on the surface of porous materials. The adsorption-desorption behavior of N_2 can therefore be used to identify the type of adsorption isotherm exhibited by the material [30]. The N_2 adsorption-desorption isotherms of CFA and SCFA are presented in Figs. 5(a) and 5(b), respectively. The results indicate that SCFA exhibits a significantly higher adsorbed volume (~293 cm^3 STP/g) compared to CFA (15.31 cm^3 STP/g) [30].

The CFA adsorption–desorption isotherms (Fig. 5(a)) exhibits a low adsorption volume (~14 cm^3 STP/g) with a gradual increase at low relative pressures and a sharp rise at higher relative pressure P/P_0, indicating limited mesoporosity and moderate surface area. In contrast, the SCFA isotherm (Fig. 5(b)) shows a pronounced adsorption increase and a clear hysteresis loop characteristic of a Type IV isotherm, confirming the presence of mesoporous structures with pore sizes in the range of 2–50 nm. The distinct hysteresis observed for SCFA suggests improved pore development and an amorphous mesoporous structure compared to CFA [31].

The SCFA materials have a BET surface area of 223 m^2/g. This indicates that SCFA has a large, specific surface area, suggesting potential as a suitable material for applications such as adsorbents, catalysts, or absorbents. The total pore volume of 0.453 cm^3/g is relatively high, indicating that the material has significant space within its structure. The average pore diameters obtained from

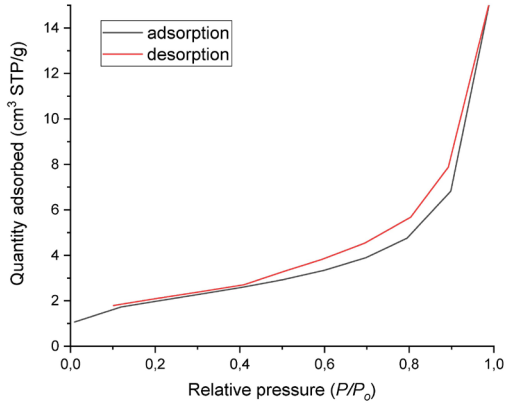

(a)

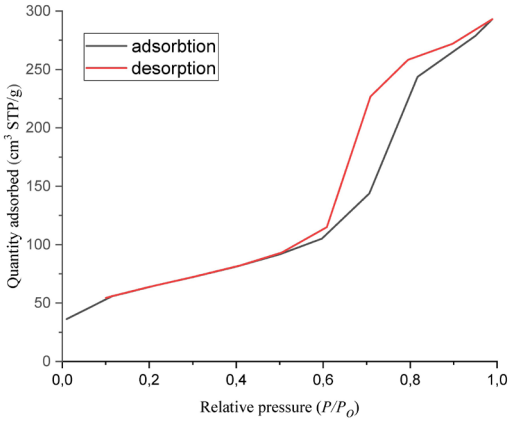

(b)

Fig. 5 (a) CFA adsorption-desorption curve; (b) SCFA adsorption-desorption curve

adsorption and desorption data using the 4V/A BET method (where V represents the total pore volume obtained from the nitrogen adsorption data and A represents the BET specific surface area, assuming cylindrical pore geometry) were 8.1 and 7.9 nm, respectively, which fall within the mesoporous size range.

The N_2 adsorption-desorption isotherms of CFA (Fig. 5(a)) exhibits transitional behavior between Type II and Type IV, characterized by a limited hysteresis loop and a pronounced uptake at high relative pressures, indicating the coexistence of mesoporous features and multilayer adsorption effects. In contrast, the SCFA sample (Fig. 5(b)) exhibits a more distinct (Type IV) isotherm with a clearer hysteresis loop. The SCFA sample shows a markedly higher adsorbed volume over the entire relative pressure range, which is consistent with its higher surface area and pore volume. These textural characteristics suggest improved accessibility of internal surfaces, making SCFA particularly suitable for applications involving adsorption, catalysis, and diffusion of relatively large molecules.

As shown in Table 7 [4, 11, 13, 32], the acid pretreatment strategy significantly affects the texture and purity of sol-gel derived silica from coal fly ash. Compared to the HCl based pretreatments reported in the literature citric acid pretreatment in this study produces silica with high purity while preserving a good balance of surface area, pore volume, and mesoporous pore size. This finding shows that citric acid is an effective and competitive pretreatment agent for producing high-quality CFA-derived silica without the need for strong mineral acids.

4 Conclusions

Silica extraction from coal fly ash was effectively optimized using response surface methodology, with optimal conditions identified as an operating temperature of 80 °C, a stirring speed of 260 rpm, and a mass-to-volume ratio of 1:4, yielding a silica yield 7.37%. The extracted silica exhibited a mesoporous structure, as confirmed by SEM and BET analyses, with a high specific surface area (≈223 m^2/g), a pore volume of 0.45 cm^3/g, and an average pore diameter of 7.8–8.1 nm, indicating its suitability as a functional porous material. This study demonstrates the potential to valorize coal fly ash into value-added silica under mild operating conditions and with citric acid-assisted pretreatment, supporting environmentally responsible waste management. The primary methodological outcome demonstrates that RSM effectively minimizes process time and energy consumption while optimizing extraction efficiency.

Analysis results, as determined by Elemental mapping and XRF, show that the material is dominated by the elements Silicon (Si) and Aluminum (Al), which are components of the main SCFAs, namely silica (SiO_2) and

Table 7 Textural comparison of sol-gel silica based on low temperature N_2 adsorption

Pretreatment agent	Surface area (m^2/g)	Pore volume (cm^3/g)	Pore diameter (nm)	Purity (%)	Reference
Citric acid	223	0.45	8.1	93	This work
HCl	497	0.49	3.1	-	[11]
HCl	290	0.40	23.3	87	[4]
HCl	225	0.43	5.8	98	[13]
HCl	110	0.38	22	-	[32]

aluminosilicate. The presence of other elements, such as Ca, Fe, and S, in small amounts indicates the existence of mineral residue from the CFA sample. Silica, with its dominance in quality, offers good structural and chemical properties, including a mesoporous structure, making SCFA a promising functional porous material for continued applications.

Acknowlegment

The author gratefully acknowledges the financial support from the National Research and Innovation Agency, Indonesia, through the Degree by Research Program, Batch 2, 2023. Appreciation is also extended to Universitas Gadjah Mada for providing academic and laboratory facilities that enabled the completion of this research.

References

[1] Aphane, M. E., Doucet, F. J., Kruger, R. A., Petrik, L., van der Merwe, E. M. "Preparation of Sodium Silicate Solutions and Silica Nanoparticles from South African Coal Fly Ash"", Waste Biomass Valorization, 11(8), pp. 4403–4417, 2020. https://doi.org/10.1007/s12649-019-00726-6

[2] Rabiul Awual, M., Munjur Hasan, M., Ihara, T., Yaita, T. "Mesoporous silica based novel conjugate adsorbent for efficient selenium(IV) detection and removal from water", Microporous and Mesoporous Materials, 197, pp. 331–338, 2014. https://doi.org/10.1016/J.Micromeso.2014.07.005

[3] Yadav, V. K., Fulekar, M. H. "Advances in methods for recovery of ferrous, alumina, and silica nanoparticles from fly ashwaste", Ceramics, 3(3), pp. 384–420, 2020. https://doi.org/10.3390/ceramics3030034

[4] Nurmalita, N., Madjid, S. N., Setiawan, A., Idroes, R., Jalil, Z. "Characteristics of Silica Powder Extracted from Fly Ash of Coal Fired Power Plant – Effect of Heat Treatment Process", Journal of Ecological Engineering, 24(9), pp. 282–292, 2023. https://doi.org/10.12911/22998993/169289

[5] Malahayati, M., Yufita, E., Ismail, I., Mursal, M., Idroes, R., Jalil, Z. "The Effect of Natural Silica from Rice Husk Ash and Nickel as a Catalyst on the Hydrogen Storage Properties of MgH_2", Journal of Ecological Engineering, 22(11), pp. 79–85, 2021. https://doi.org/10.12911/22998993/142959

[6] Malahayati, M., Ismail, I., Mursal, M., Jalil, Z. "The use of silicon oxide extracted from rice husk ash as catalyst in magnesium hydrides (MgH_2) prepared by mechanical alloying method", Journal of Physics: Conference Series, 1120(1), 012061, 2018. https://doi.org/10.1088/1742-6596/1120/1/012061

[7] Sitohang, C., Kuncaka, A., Suratman, A. "Synthesis of Mesoporous Silica from Palm Oil Boiler Ash (MS-POBA) with Addition of Methyl Ester Sulfonate as a Template for Free Fatty Acid Adsorption from Crude Palm Oil (CPO)", Indonesian Journal of Chemistry, 24(3), pp. 729–741, 2024. https://doi.org/10.22146/ijc.87703

[8] Kócs, L., Albert, E., Tegze, B., Kabai-Faix, M., Major, C., Szalai, A., Basa, P., Hórvölgyi, Z. "Silica Sol-gel coatings with improved light transmittance and stability", Periodica Polytechnica Chemical Engineering, 62(1), pp. 21–31, 2018. https://doi.org/10.3311/PPch.10550

[9] Darwis, D., Khaeroni, R., Iqbal, I. "Purification and Characterization of Silica Using Purification (Leaching) Method with Variations of Milling Time from Quartz Sand on Pasir Putih Village South Pamona Sub-district of Poso District", Natural Science: Journal of Science and Technology, 6(2), pp. 187–193, 2017.

[10] De Oliveira, F. F., Moura, K. O., Costa, L. S., Vidal, C. B., Loiola, A. R., Do Nascimento, R. F. "Reactive Adsorption of Parabens on Synthesized Micro- And Mesoporous Silica from Coal Fly Ash: PH Effect on the Modification Process", ACS Omega, 5(7), pp. 3346–3357, 2020. https://doi.org/10.1021/acsomega.9b03537

[11] Yuan, N., Cai, H., Liu, T., Huang, Q., Zhang, X. "Adsorptive removal of methylene blue from aqueous solution using coal fly ash-derived mesoporous silica material", Adsorption Science & Technology, 37(3–4), pp. 333–348, 2019. https://doi.org/10.1177/0263617419827438

[12] Li, C.-C., Qiao, X.-C. "A new approach to prepare mesoporous silica using coal fly ash", Chemical Engineering Journal, 302, pp. 388–394, 2016. https://doi.org/10.1016/j.cej.2016.05.029

[13] Zewide, Y. T., Yemata, T. A., Ayalew, A. A., Kedir, H. J., Tadesse, A. A., …, Mihiret, M. T. "Application of response surface methodology (RSM) for experimental optimization in biogenic silica extraction from rice husk and straw ash", Scientific Reports, 15(1), 132, 2025. https://doi.org/10.1038/s41598-024-83724-6

[14] Matlob, A. S., Kamarudin, R. A., Jubri, Z., Ramli, Z. "Using the Response Surface Methodology to Optimize the Extraction of Silica and Alumina from Coal Fly Ash for the Synthesis of Zeolite Na-A", Arabian Journal for Science and Engineering, 37(1), pp. 27–40, 2012. https://doi.org/10.1007/s13369-011-0149-2

[15] Aprilia, S., Rosnelly, C. M., Zuhra, Z., Fitriani, F., Haffiz Akbar, E., Raqib, M., Rahmah, K., Amin, A., Baity, R. A. "Synthesis of amorphous silica from rice husk ash using the sol-gel method: Effect of alkaline and alkaline concentration", Materials Today: Proceedings, 87, pp. 225–229, 2023. https://doi.org/10.1016/J.MATPR.2023.02.403

[16] Silviana, S., Sanyoto, G. J., Darmawan, A., Sutanto, H. "Geothermal silica waste as sustainable amorphous silica source for the synthesis of silica xerogels", Rasayan Journal of Chemistry, 13(3), pp. 1692–1700, 2020. https://doi.org/10.31788/RJC.2020.1335701

[17] Made Joni, I., Rukiah, R., Panatarani, C. "Synthesis of silica particles by precipitation method of sodium silicate: Effect of temperature, pH and mixing technique", AIP Conference Proceedings, 2219(1), 080018, 2020. https://doi.org/10.1063/5.0003074

[18] Simatupang, L., Siburian, R., Sitanggang, P., Doloksaribu, M., Situmorang, M., Marpaung, H. "Synthesis and application of silica gel base on mount Sinabung's fly ash for Cd(II) removal with fixed bed column", Rasayan Journal of Chemistry, 11(2), pp. 819–827, 2018.
https://doi.org/10.31788/RJC.2018.1122091

[19] Zainol, N., Aziz, N. H., Jazlan, C. A. I. C., Razahazizi, N. A. "The Application of Design of Experiments in the Hatchery Wastewater Treatment through Biological Method", Current Applied Science and Technology, 23(2), 2023.
https://doi.org/10.55003/cast.2022.02.23.003

[20] Cendekia, D., Ayu Afifah, D., Hanifah, W. "Linearity Graph in the Prediction of Granular Active Carbon (GAC) Adsorption Ability", IOP Conference Series: Earth and Environmental Science, 1012, 012079, 2021.
https://doi.org/10.1088/1755-1315/1012/1/012079

[21] Geow, C. H., Tan, M. C., Yeap, S. P., Chin, N. L. "A Review on Extraction Techniques and Its Future Applications in Industry", European Journal of Lipid Science and Technology, 123(4), 2000302, 2021.
https://doi.org/10.1002/ejlt.202000302

[22] Salamah, S., Trisunaryanti, W., Kartini, I., Purwono, S. "Synthesis of Mesoporous Silica from Beach Sand by Sol-Gel Method as a Ni Supported Catalyst for Hydrocracking of Waste Cooking Oil", Indonesian Journal of Chemistry, 22(3), pp. 726–741, 2022.
https://doi.org/10.22146/ijc.70415

[23] Alvita, L. R., Elsyana, V., Kining, E. "Optimization Of The Hydrolysis Process Of Microalgae Porphyridium Cruentum Biomass With Variations Of Hydrochloric Acid (Hcl) Concentration, Temperature, And Time Using Response Surface Methodology (RSM)", Alchemy: Journal Of Chemistry, 11(2), pp. 51–56, 2023.
https://doi.org/10.18860/al.v11i2.19500

[24] Buhani, B., Rinawati, R., Suharso, S., Yuliasari, D. P., Yuwono, S. D. "Removal of Ni(II), Cu(II), and Zn(II) ions from aqueous solution using Tetraselmis sp. biomass modified with silica-coated magnetite nanoparticles", Desalination and Water Treatment, 80, pp. 203–213, 2017.
https://doi.org/10.5004/dwt.2017.20932

[25] Imoisili, P. E., Jen, T. C. "Microwave-assisted sol-gel template-free synthesis and characterization of silica nanoparticles obtained from South African coal fly ash", Nanotechnology Reviews, 11(1), pp. 3042–3052, 2022.
https://doi.org/10.1515/ntrev-2022-0476

[26] Imoisili,P. E., Ukoba, K. O., Jen, T. C. "Green technology extraction and characterisation of silica nanoparticles from palm kernel shell ash via sol-gel", Journal of Materials Research and Technology, 9(1), pp. 307–313, 2020.
https://doi.org/10.1016/J.JMRT.2019.10.059

[27] Awadh, S. M., Yaseen, Z. M. "Investigation of silica polymorphs stratified in siliceous geode using FTIR and XRD methods", Materials Chemistry and Physics, 228, pp. 45–50, 2019.
https://doi.org/10.1016/J.MATCHEMPHYS.2019.02.048

[28] Imoisili, P. E., Jen, T.-C. "Synthesis and characterization of amorphous nano silica from South African coal fly ash", Materials Today: Proceedings, 105, pp. 21–26, 2024.
https://doi.org/10.1016/J.MATPR.2023.06.077

[29] Manyepedza, T., Gaolefufa, E., Beas, I. N., Kabomo, M. T., Modukanele, B. "High-Purity Template-Free Mesoporous Silica Synthesized From Coal Fly Ash", ChemistrySelect, 9(8), e202305065, 2024.
https://doi.org/10.1002/slct.202305065

[30] Kalam, S., Abu-Khamsin, S. A., Kamal, M. S., Patil, S. "Surfactant Adsorption Isotherms: A Review", ACS Omega, 6(48), pp. 32342–32348, 2021.
https://doi.org/10.1021/acsomega.1c04661

[31] Rahman, M. M., Shafiullah, A. Z., Pal, A., Islam, M. A., Jahan, I., Saha, B. B. "Study on optimum iupac adsorption isotherm models employing sensitivity of parameters for rigorous adsorption system performance evaluation", Energies, 14(22), 7478, 2021.
https://doi.org/10.3390/en14227478

[32] Gómez M., Pizarro, J., Díaz, C., Ortiz, C., Castillo, X., Navlani-García, M., Cazorla-Amorós, D. "Silica extracts from fly ash modified via sol-gel methods and functionalized with CMPO for potential scavenging of rare earth elements La^{3+} and Ce^{3+}", Materials Chemistry and Physics, 318, 129161, 2024.
https://doi.org/10.1016/j.matchemphys.2024.129161